

21

A TRIDENT SCHOLAR PROJECT REPORT

NO. 220

AD-A284 858



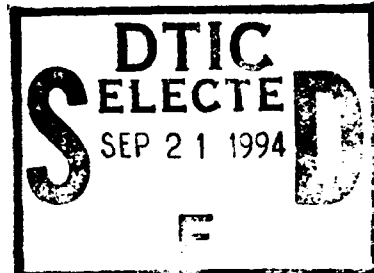
"Motor Current Signal Analysis for Diagnosis of
Fault Conditions in Shipboard Equipment"



94-30333



SPS



UNITED STATES NAVAL ACADEMY
ANNAPOLIS, MARYLAND

DTIC QUALITY INSPECTED 3

This document has been approved for public
release and sale; its distribution is unlimited.

94 9 20 067

U.S.N.A.-- Trident Scholar project report; no. 220 (1994)

**"Motor Current Signal Analysis for Diagnosis of
Fault Conditions in Shipboard Equipment"**

by
Midshipman Jonathan Adam Siegler, Class of 1994
U.S. Naval Academy
Annapolis, Maryland

Antal A. Sarkady
Advisor: Professor Antal A. Sarkady
Electrical Engineering Department

Accepted for Trident Scholar Committee

Francis D'Correll
Chair

19 May 1994
Date

Accession For	
NTIS	CRAB
DTIC	TAB
Unpublished	
Justification	
By	
Distribution/	
Availability Codes	
Dist	Avail and/or Special
A-1	

REPORT DOCUMENTATION PAGE

Form Approved
OMB no. 0704-0188

Public reporting burden for this collection of information is estimated to average 1 hour of response, including the time for reviewing instructions, searching existing data sources, gathering and maintaining the data needed, and completing and reviewing the collection of information. Send comments regarding this estimate or any other aspect of the collection of information, including suggestions for reducing burden, to Department of Defense, Defense Program Evaluation and Assessment, 1215 Jefferson Davis Highway, Suite 1200, Arlington, VA 22202-4302, and to Office of Management and Budget, Paperwork Reduction Project (0704-0188), Washington, DC 20585.

1. AGENCY USE ONLY (Leave blank)	2. REPORT DATE	3. REPORT TYPE AND DATES COVERED	
	19 May 1994		
4. TITLE AND SUBTITLE Motor current signal analysis for diagnosis of fault conditions in shipboard equipment			5. FUNDING NUMBERS
6. AUTHOR(S) Jonathan Adam Siegler			
7. PERFORMING ORGANIZATION'S NAME(S) AND ADDRESS(ES) U.S. Naval Academy, Annapolis, MD			8. PERFORMING ORGANIZATION REPORT NUMBER USNA Trident Scholar project report; no. 220 (1994)
9. SPONSORING/MONITORING AGENCY NAME(S) AND ADDRESS(ES)			10. SPONSORING/MONITORING AGENCY REPORT NUMBER
11. SUPPLEMENTARY NOTES Accepted by the U.S. Trident Scholar Committee			
12a. DISTRIBUTION/AVAILABILITY STATEMENT This document has been approved for public release; its distribution is UNLIMITED.		12b. DISTRIBUTION CODE	
13. ABSTRACT (Maximum 200 words) Motor Current Signal Analysis is a technique for diagnosing problems in mechanical equipment by monitoring nothing more than the input electrical signal. The induction motor acts as a bilateral transducer, converting mechanical vibrations into electrical signal perturbations. It provides a method for a non-invasive testing of mechanical systems. The objective of this project was to develop the signal processing routines and classification techniques necessary to implement this method of fault detection. Data were collected from a Byron Jackson Main Sea Water Pump found on a U.S. submarine. The fault that was monitored was an eroded impeller condition. This project not only provides a method for detecting this specific fault condition, but furnishes the groundwork for the development of test equipment to completely monitor the pump's operation.			
DTIC QUALITY LEVEL 3			
14. SUBJECT TERMS Motor current signal analysis, fault detection, fault monitoring, marine mechanical equipment			15. NUMBER OF PAGES
			16. PRICE CODE
17. SECURITY CLASSIFICATION OF REPORT UNCLASSIFIED	18. SECURITY CLASSIFICATION OF THIS PAGE UNCLASSIFIED	19. SECURITY CLASSIFICATION OF ABSTRACT UNCLASSIFIED	20. LIMITATION OF ABSTRACT UNCLASSIFIED

Abstract

In the Navy it is imperative that systems and equipment work at their peak performance levels. Man-hours, money, and even lives may depend on it. On a submarine, it may even be more important, because fault conditions in equipment can lead to increased noise levels, and form a higher probability of detection by the enemy. There are inherent problems associated with detecting fault conditions in shipboard equipment. Most importantly, equipment must often be shut down, and taken apart. This can cost countless man-hours, and down time that an underway vessel cannot afford. In addition, the equipment may be located in an area that is very difficult or impossible to reach under normal circumstances. This would include all equipment found in the primary plant of a nuclear powered submarine.

Motor current signal analysis provides a solution to these problems. It is a non-invasive technique for monitoring and diagnosing mechanical problems associated with equipment driven by electrical motors. The objective of this project was to implement this process by (1) examining the electrical power signal supplied to a Byron Jackson sea water pump found in a U.S. submarine and (2) to develop signal processing routines and classification techniques to distinguish between the pump working with a good impeller and the pump working with an eroded impeller. Although this one fault condition was studied, this research sought to develop a method by which other fault conditions could be detected.

Key Word Search: signal processing pattern recognition

Preface

This project was both suggested and sponsored by the Submarine Monitoring, Maintenance, and Support Office (SMMSO). I would specifically like to thank Ed Farino (Code # PMS 390) for making this project possible. Furthermore, all the equipment and instrumentation associated with the data collection were provided by the Carderock Division of the Naval Surface Warfare Center, Annapolis, Maryland. I would like to thank the project engineer Chris Nemarich, the electrical engineer Diane Porter, and the electrical technician Dave Kosick (Code # 853).

Contents

	Introduction	4
Chapter 1	Data Collection and the Physical Apparatus	7
1.1	The Byron Jackson Sea Water Pump	7
1.2	The Eroded Impeller Condition	9
1.3	Data Acquisition	9
1.4	Data Transfer	11
Chapter 2	Digital Demodulation	12
2.1	The Hilbert Transform	12
2.2	The Analytic Signal	13
2.3	Implementation on the Computer	16
Chapter 3	Ensemble Averaging	23
3.1	The Original Signal	23
3.2	Partitioning the Signal	25
3.3	The Averaging Process	26
3.4	Improving the Signal-to-Noise Ratio	29
Chapter 4	Processing the Power Signal	30
4.1	The Initial Analysis	30
4.2	The Application of Ensemble Averaging to the Undemodulated Spectrum	34
4.3	The Application of the Analytic Signal	36
Chapter 5	Determination of the Pump Condition	39
5.1	Pinpointing the Rugged Signal Features	39
5.2	The 1% Test	41
5.3	The Moving Average Filter	43
5.4	Creating the Pattern Vector	44
5.5	The Nearest Neighborhood Technique	45
5.6	The Perceptron	47
	The Future	51
	Works Cited	52

Introduction

The art of signal processing can be implemented in many applications outside the normal field of electrical engineering. If a physical process produces a signal that can be sampled in time with a sufficiently high rate to preserve the information content, a powerful set of computer based digital signal processing tools can be applied to the problem. From diagnosing a heart condition, to finding flaws in a metal weld, signal processing techniques can provide invaluable information about the process. In this project, signal processing routines were implemented to detect fault conditions in a Navy pump.

In the Navy it is imperative that systems and equipment work at their peak performance levels. Man-hours, money, and even lives may depend on it. On a submarine it may be even more important, because fault conditions in equipment can lead to increased noise levels, and form a higher probability of detection by the enemy. There are inherent problems though, associated with detecting fault conditions in shipboard equipment. Most importantly, equipment must often be shut down, and taken apart to be examined. This can cost countless man-hours and down time that an underway vessel cannot afford. Also, the equipment may be located in an area of the vessel that is very difficult or impossible to reach under normal circumstances. This would include all

equipment found in the primary plant of a nuclear powered submarine.

The equipment must be monitored periodically, because these fault conditions reduce efficiency, and can possibly lead to the complete destruction of the system. This creates a significant dilemma for a vessel. On the one hand, monitoring these conditions is time consuming and expensive. On the other hand, the failure to monitor these conditions can lead to inefficient operation and the possibility of extended time in dry dock. In the past a compromise had to be made. Today, with the development of relatively inexpensive and powerful computers this compromise is no longer necessary.

Motor Current Signal Analysis is a technique for diagnosing problems in mechanical equipment by monitoring nothing more than the input electrical signal. The induction motor acts as a bilateral transducer, converting mechanical vibrations into electrical signal perturbations. It provides a method for a non-invasive testing of mechanical systems. It is an efficient and inexpensive solution to the Navy's problem. It provides a means to detect fault conditions while the equipment is still in operation. Also, since this technique only requires access to the electrical signal, it can be implemented with any remote electro-mechanical equipment whose power lines can be monitored. This would include a large set of equipment on a

Navy vessel.

The objective of this project was to develop the signal processing routines and classification techniques necessary to implement this method of fault detection. Data were collected from a Byron Jackson Sea Water Pump found on a U.S. submarine. The fault that was monitored was an eroded impeller condition. This project not only provides a method for detecting this specific fault condition, but furnishes the groundwork for the development of test equipment to completely monitor the pump's operation.

Chapter One

Data Collection and the Physical Apparatus

The first step in the project was to gather electrical data from the Byron Jackson Sea Water Pump. The data were in the form of a sampled time series that would later be applied to a signal processing scheme in an off-line mode.

1.1 The Byron Jackson Sea Water Pump

The Byron Jackson Sea Water Pump is a centrifugal pump that can be found on a U.S. submarine. The actual mock-up used to conduct the tests was located at the Carderock Division of the Naval Surface Warfare Center, Annapolis,

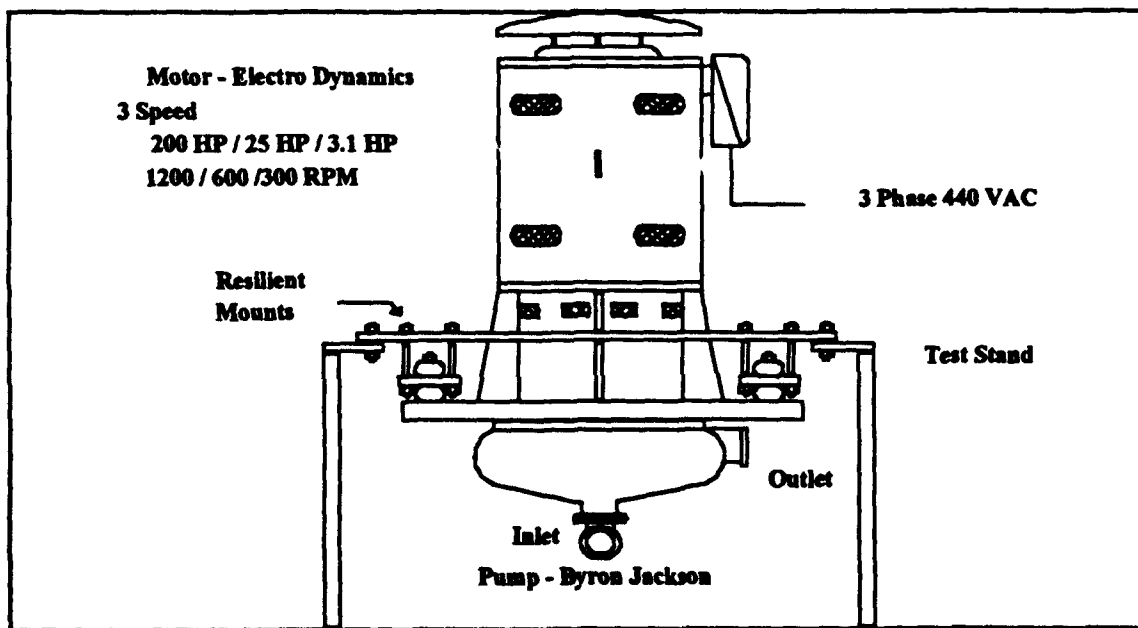


Figure 1.1-The Byron Jackson Sea Water Pump

Maryland. The pump is shown in Figure 1.1. It is a centrifugal pump driven by a three phase, 60 Hz, 440 Vac induction motor. For this project, the tests were conducted under fast speed, 1200 RPM, and under high suction pressure. Tests were conducted using both impellers in good condition, and impellers in the eroded condition.

A cross sectional view of a typical centrifugal pump is shown below in Figure 1.2. The suction pressure is developed by the vanes on the rotating impeller. As the

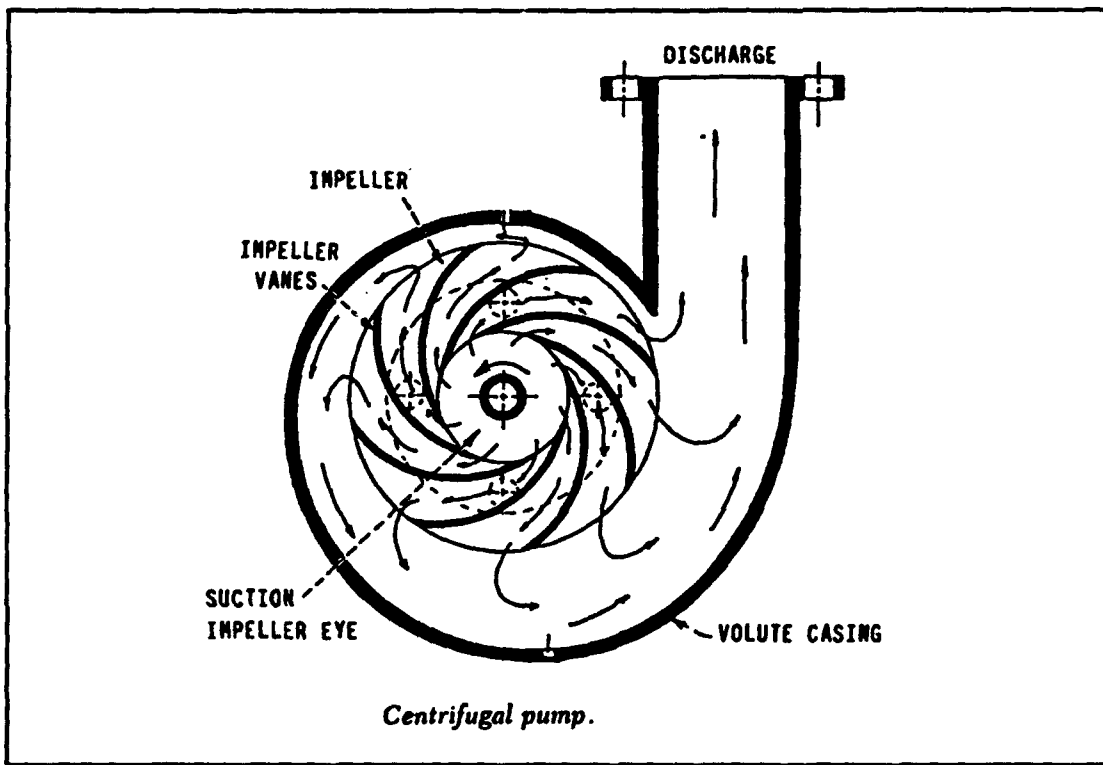


Figure 1.2-A typical centrifugal pump

impeller rotates about the center shaft, a pressure differential develops between the suction impeller eye and the volute casing. Since the tips of the vanes are moving faster than the center of the impeller, the Venturi Effect

dictates that a suction will develop towards the outside of the pump at the volute casing (Munson 135). Consequently, the fluid is forced out the discharge pipe.

1.2 The Eroded Impeller Condition

Over its operating life, the impeller spins at various speeds for long periods of time. As time passes its original smooth finish becomes corrupted with grooves and corrugations. These can lead to both inefficient operation and increased noise levels. Since the impeller may become unbalanced, this condition may induce vibrations that can damage the entire pump.

The eroded condition will affect the amount of torque provided by the three phase induction motor. The torque produced at the impeller is proportional to the power used by the motor. It was postulated that changes in the torque due to the eroded impeller condition would lead to changes in the input power driving the induction motor. In other words, the reflected load variations from the pump would allow the fault to be detected in the power signal.

1.3 Data Acquisition

To implement this fault detection system, the power signal would have to be recorded and digitally stored. The analog equipment in Figure 1.3 was used to obtain the real

power signal. The equipment was placed at the electrical inputs to the three phase induction motor. Basically, the individual, analog phase voltages were multiplied by their corresponding phase currents to get the individual phase power signals. Because analog multipliers were used, nonlinearities were introduced into the signals. These were dealt with when the signals were later processed. The individual phase voltages were then added together to get the total instantaneous real power signal (P).

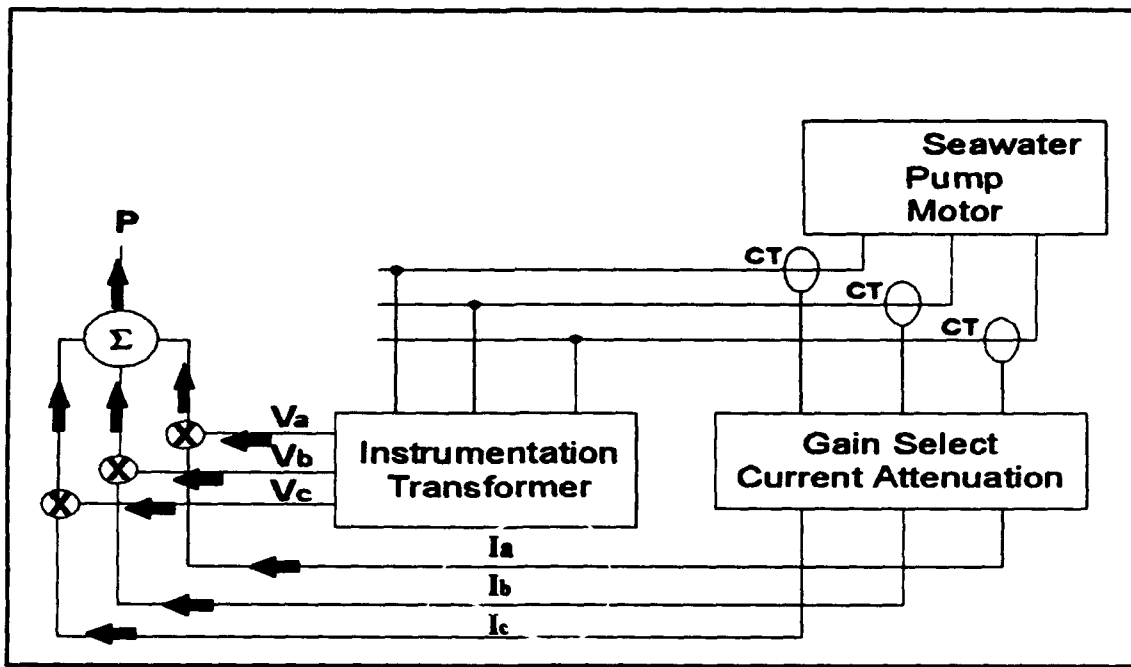


Figure 1.3-Instrumentation used to obtain real power (P)

This real power signal (P) now had to be digitized and stored for later processing. In order to sample a signal without aliasing it, the highest frequency component of the signal must be less than half of the sampling frequency (The Nyquist Criteria) (Stremler 129). The analog signal (P) was

first applied to a precision analog low-pass filter with a cut-off frequency of approximately 2900 Hz. This cut-off frequency was chosen because the information was found to be bandwidth limited to this interval. A sampling frequency of 6000 Hz was chosen to satisfy the Nyquist criterion. The signal was then digitally sampled and recorded using a digital tape recorder. The data were quantized by an analog to digital converter with a 90 dB dynamic range(16 bits). Each digital data segment was 2 minutes in duration.

This acquisition process was used to record the power signals from both impellers in good condition and impellers in the eroded condition. Twelve 2 minute samples were taken using eroded impellers, and eight samples were recorded using good impellers.

1.4 Data Transfer

HP Basic routines, provided by the Naval Surface Warfare Center, were used to transfer the data to the computer for later processing. The digital data were transported through an HPIB bus into binary files on the computer. These binary files were then converted into MATLAB .dat-files. The data were now ready to be processed.

Chapter 2

Digital Demodulation

The operation of a centrifugal pump centers around the rotation of the impeller vanes. An impeller in good condition would tend to be balanced and function smoothly. The eroded impeller condition though, would cause vibrations that would be superimposed on the normal rotation. This can be seen intuitively as a type of modulation process. It was hypothesized that this modulation property would be apparent in the power signal. To exploit this characteristic, the analytic signal was formed and used to digitally demodulate the power data. The first step in the formation of the analytic signal is the application of the Hilbert Transform.

2.1 The Hilbert Transform

If $s(t)$ is a real signal, then the Hilbert transform (Stremler 260) is defined as the convolution of $s(t)$ by $(1/\pi*t)$:

$$s_h(t) = s(t) * \left(\frac{1}{\pi \cdot t} \right) = \frac{1}{\pi} \cdot \int_{-\infty}^{\infty} s(\lambda) \cdot \frac{1}{t - \lambda} d\lambda \quad 2.1$$

After taking the Fourier Transform (Stremler 84) of $s_h(t)$, and shifting to the frequency domain, we obtain:

$$F(s_h(t)) = S_h(\omega) = S(\omega) \cdot F\left(\frac{1}{\pi \cdot t}\right) \quad 2.2$$

and,

$$F\left(\frac{1}{\pi \cdot t}\right) = \frac{1}{\pi} \cdot \int_{-\infty}^{\infty} \frac{1}{t} \cdot e^{-j\omega t} dt = -j \cdot \text{sgn}(\omega) \quad 2.3$$

where F is the Fourier Transform operator, and $\text{sgn}(\omega)$ is defined as: $\text{sgn}(\omega) = 1$ for $\omega > 0$, 0 for $\omega = 0$ and -1 for $\omega < 0$. Thus,

$$\begin{aligned} S_h(\omega) &= (-j \cdot \text{sgn}(\omega)) \cdot S(\omega) = -j \cdot S(\omega) && \text{for } \omega > 0 \\ & & & \quad j \cdot S(\omega) && \text{for } \omega < 0 \\ & & & \quad 0 & & \text{for } \omega = 0 \end{aligned} \quad 2.4$$

The Hilbert Transform is known as a quadrature function because each component of $S_h(\omega)$ is in phase quadrature with $S(\omega)$. In other words, the frequency components are 90 degrees out of phase with the original spectrum. Using the Hilbert Transform of $s(t)$, the analytic signal can be formed and used to digitally demodulate the power signal.

2.2 The Analytic Signal

We define a complex function $z(t)$, the analytic signal, derived from the information carrying signal $s(t)$ as:

$$z(t) = s(t) + j \cdot s_h(t) \quad 2.5$$

It is important to note that, while $s(t)$ is a signal that

exists in the real world, $z(t)$ is a contrived, complex signal that exists only in the mind and on the computer.

After taking the Fourier Transform of the analytic signal, and moving to the frequency domain:

$$F(z(t)) = Z(\omega) = S(\omega) + j \cdot S_h(\omega) = S(\omega) + j \cdot (-j \cdot \text{sgn}(\omega)) \cdot S(\omega) \quad 2.6$$

From Equation 2.4,

$$\begin{aligned} Z(\omega) &= S(\omega) \cdot (1 + \text{sgn}(\omega)) = 2 \cdot S(\omega) & \text{for } \omega > 0 \\ &= S(\omega) & \text{for } \omega = 0 \\ &= 0 & \text{for } \omega < 0 \end{aligned} \quad 2.7$$

Thus, $Z(\omega)$ is an upper single-sidebanded signal in the baseband. In other words, it is created by zeroing the negative side of the original frequency spectrum, and doubling the positive side, excluding the DC component. This same technique is used to produce single-sideband modulation.

If we start with a real, large carrier, amplitude modulated, and/or angle modulated signal $s(t)$:

$$s(t) = a(t) \cdot \cos(\omega_c t + \phi(t)) \quad 2.8$$

where $a(t)$ is the amplitude modulating signal

$\phi(t)$ is the angle modulating signal

ω_c is the carrier frequency

it can be shown that $z(t)$ is of the form:

$$z(t) = s(t) + j \cdot s_h(t) = a(t) \cdot \cos(\omega_c t + \phi(t)) + j \cdot a(t) \cdot \sin(\omega_c t + \phi(t)) \quad 2.9$$

$$z(t) = a(t) \cdot e^{j \cdot (\omega_c t + \phi(t))} \quad 2.10$$

At this point it is easy to see that $z(t)$ is a complex representation of the original signal $s(t)$. Although it does not exist in the real world, it can provide valuable insight into the original signal $s(t)$.
Taking the absolute value and phase of $z(t)$:

$$|z(t)| = |a(t)| \cdot \left| e^{j(\omega_c t + \phi(t))} \right| = |a(t)| \cdot 1 = |a(t)| \quad 2.11$$

$$\text{Ph}(z(t)) = \theta(t) = \arctan\left(\frac{\text{Im}(z(t))}{\text{Re}(z(t))}\right) = \omega_c t + \phi(t) \quad 2.12$$

From Equation 2.11 it is easy to see that the absolute value of $z(t)$ produces the amplitude modulation $a(t)$. The phase of $z(t)$ leads to the sum of the carrier signal and the angle modulation $\phi(t)$. A linear regression could be used to remove the straight line carrier and retrieve the angle

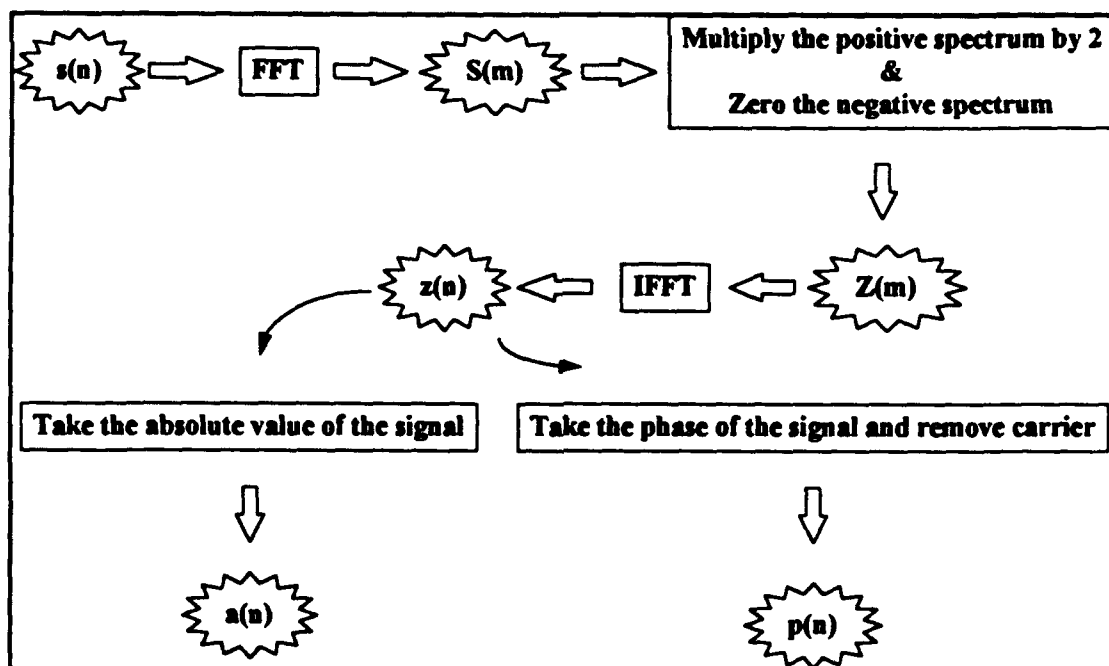


Figure 2.1-The algorithm to implement the analytic signal on the computer

modulation from the phase signal. The FM modulation could be found by taking the derivative of the angle modulation. In other words, the analytic signal provides a method to AM, PM, and FM demodulate the original signal $s(t)$.

2.3 Implementation on the Computer

To form the analytic signal on the computer, the algorithm described in Figure 2.1 was employed. First, the Fast Fourier Transform(Hush 102) was applied to the original sampled time series $s(n)$. Then, the analytic signal was formed by doubling the positive side of the spectrum (excluding the DC term), $S(m)$, and zeroing the negative side of the spectrum. Now, the Inverse Fast Fourier Transform was applied, producing the time domain representation of the complex analytic signal $z(n)$.

The original AM modulation could be found by taking the absolute value of the analytic signal. The phase of the analytic signal produced the sum of the carrier signal and the angle modulation. The carrier signal was then subtracted, leaving only the phase modulation.

This system could be used to demodulate any digitally sampled signal. For instance, if either a double sideband large carrier AM or FM radio broadcast was digitally sampled and stored, this process could be used to demodulate the signal. The demodulated signal could then be applied to a digital to analog converter and played through a speaker.

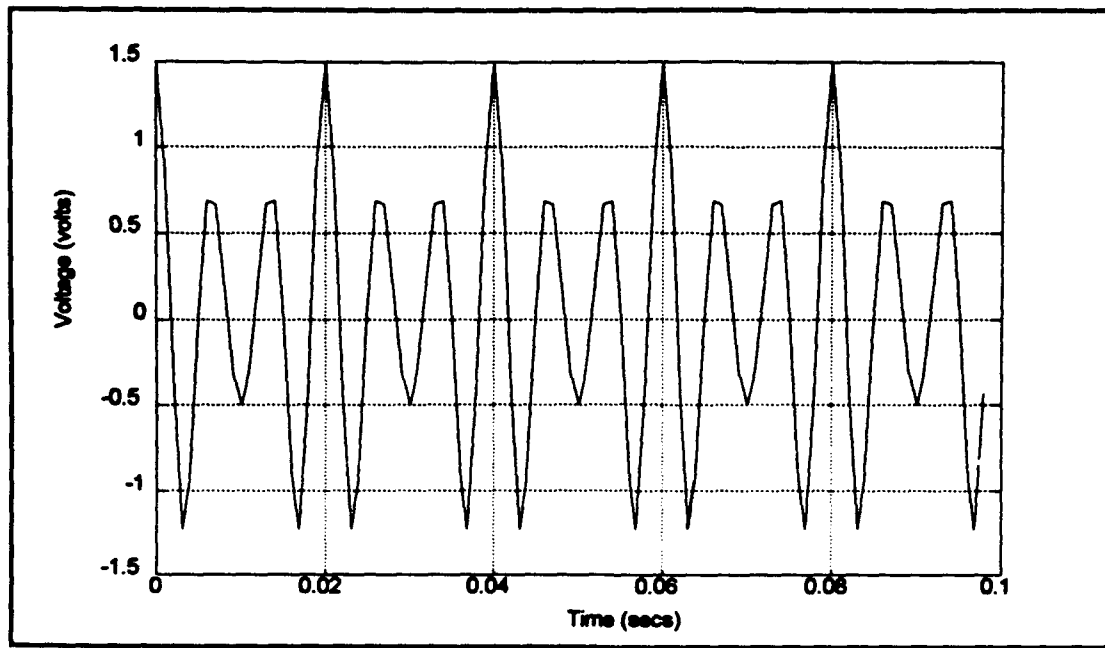


Figure 2.2-A large carrier double sideband AM modulated signal (Carrier=150 Hz Modulation=50 Hz)

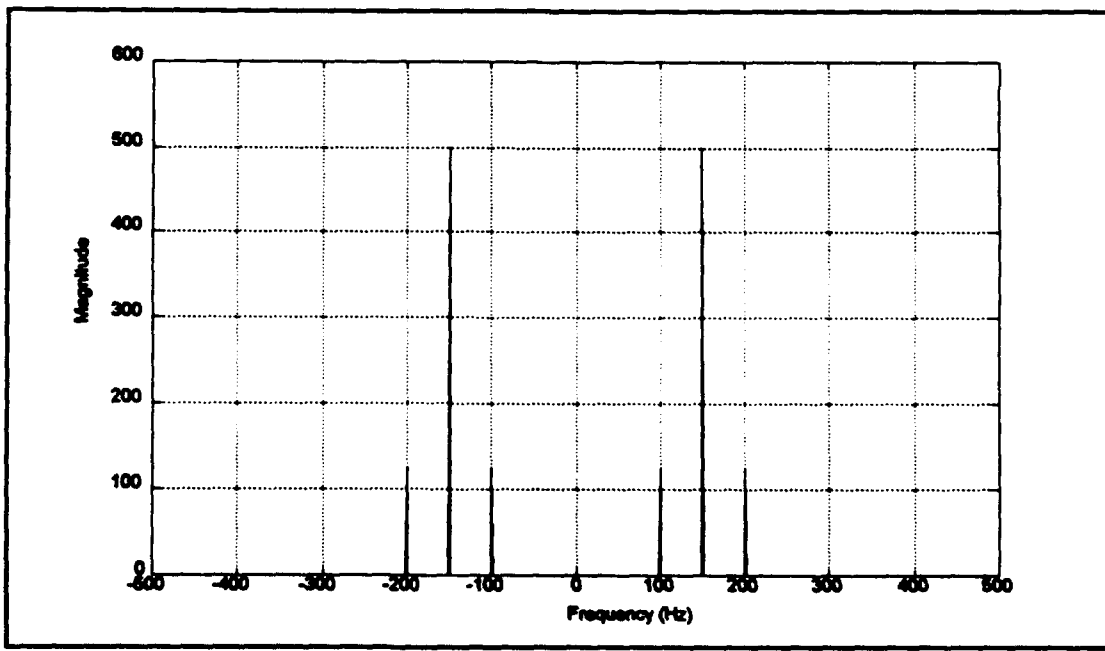


Figure 2.3-The magnitude spectrum of the AM signal

Figures 2.2 and 2.3 show an amplitude modulated signal and its corresponding frequency spectrum. These help to illustrate the power of the analytic signal. In the spectrum, it is important to note that the 50 Hz base band information has been shifted about the carrier at 150 Hz.

After forming the analytic signal, the absolute value was taken to AM demodulate the signal. From Figures 2.4 and 2.5 it is easy to see that the signal has in fact been AM demodulated, and the information is back in the base band at 50 Hz.

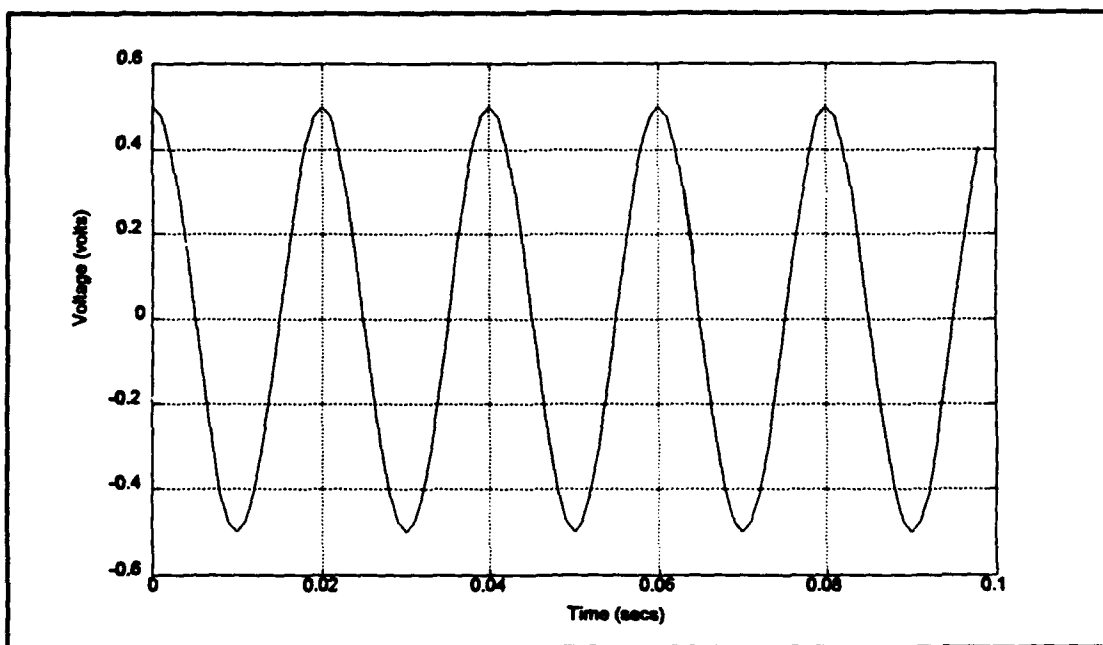


Figure 2.4-The AM demodulated signal

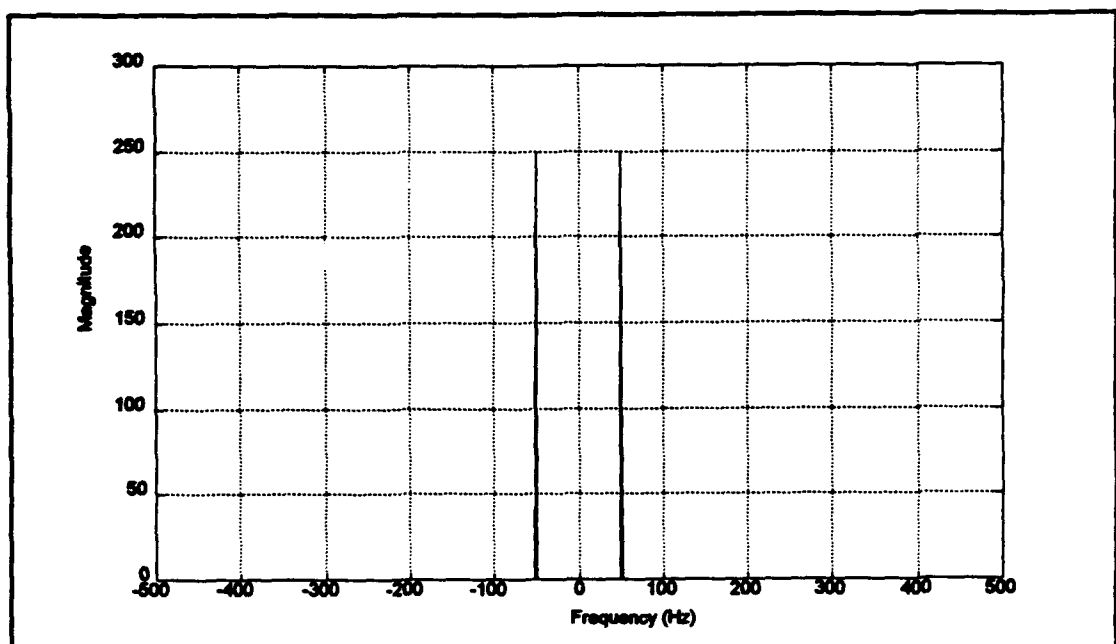


Figure 2.5-The magnitude spectrum of the AM demodulated signal

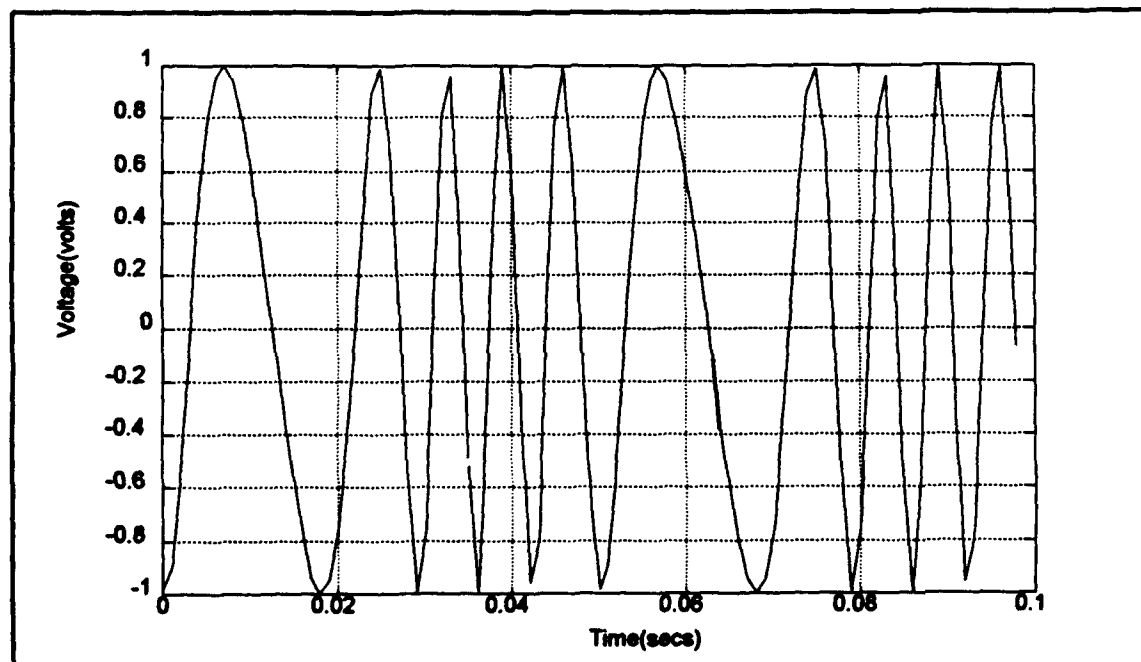


Figure 2.6-An angle modulated signal (Carrier=100 Hz
Modulation=20 Hz $\beta=3$)

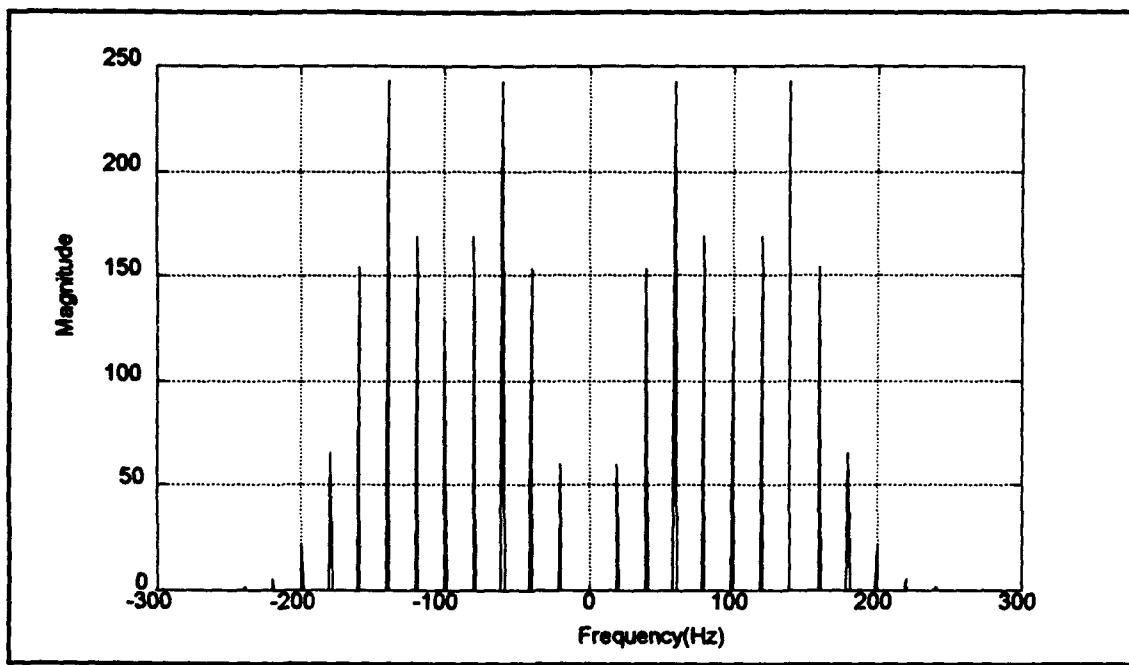


Figure 2.7-The magnitude spectrum of the angle modulated signal

A similar result occurs with an angle modulated signal. Figures 2.6 and 2.7 show the time and frequency domain representations of an angle modulated signal. The energy in the signal is centered around the carrier at 100 Hz and shifted off the carrier at multiples of the modulating frequency. The energy shift follows a first order Bessel function with $\beta=3$.

The analytic signal was formed, and its phase was calculated. After fitting a linear regression curve to the signal and subtracting the carrier, the 20 Hz of angle modulation remained (Figure 2.8). Figure 2.9 shows that the energy has been translated back into the base band at 20 Hz.

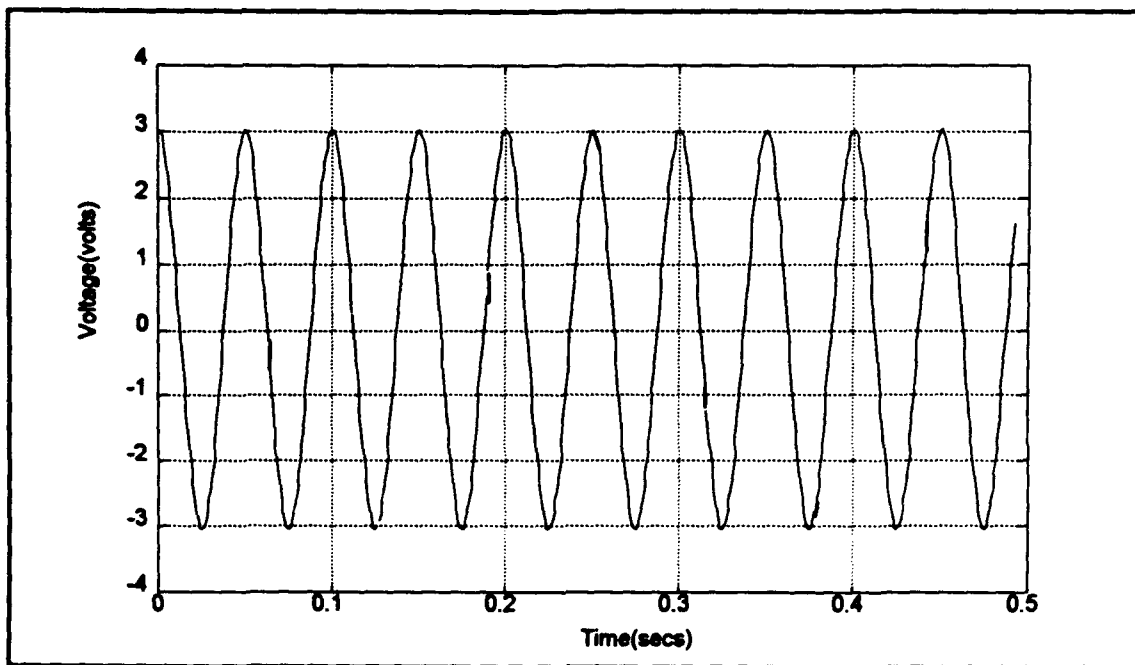


Figure 2.8-The angle demodulated signal

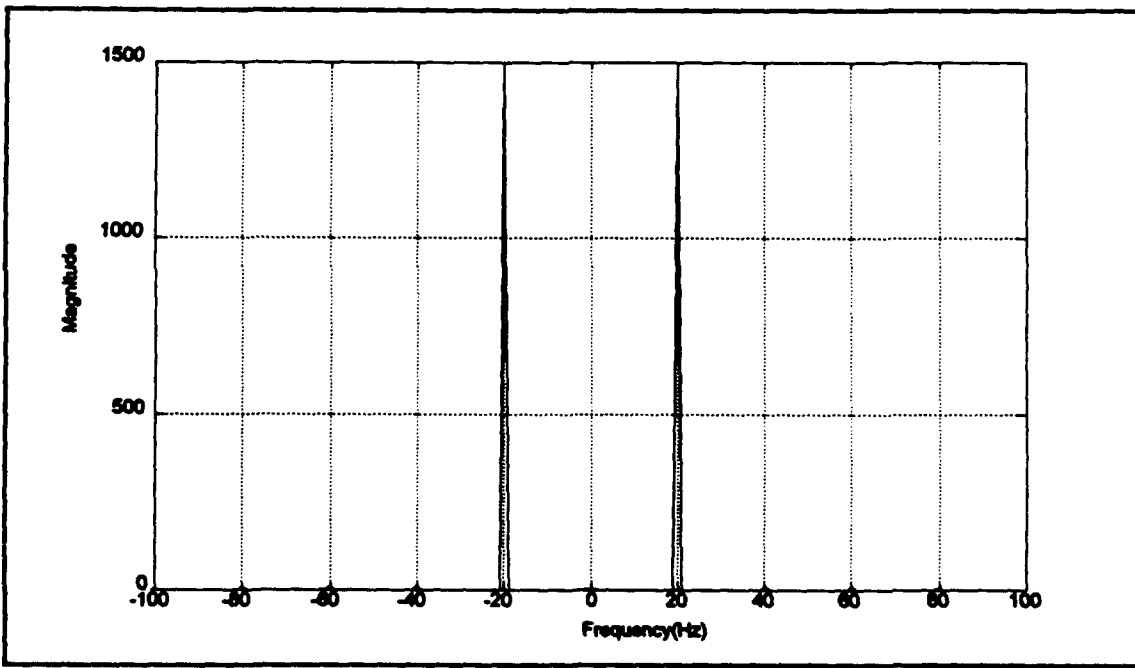


Figure 2.9-The magnitude spectrum of the angle demodulated signal

Consequently, the analytic signal provides an efficient method for a computer to digitally AM, PM and FM demodulate a sampled time series. This method can give further insight into a signal that exhibits these modulation properties. This process was used to demodulate the real power signal recorded during the trials.

Chapter 3

Ensemble Averaging

Often a real signal is composed of an information carrying signal (ICS) masked in random Gaussian noise. If the signal-to-noise ratio is high, a single Fourier spectral estimate is sufficient to detect spectral lines in the computed frequency spectrum. If the signal-to-noise ratio is poor, then several spectral estimates must be ensemble averaged to aid in the detection. The technique of data segmentation and ensemble averaging is known as the Bartlett smoothing procedure (Jenkins 255). This technique can be used to detect spectral lines buried in additive Gaussian noise even with extremely poor signal-to-noise ratios.

3.1 The Original Signal

Suppose we are given a signal $f(t)$, composed of an information carrying signal $s(t)$, masked heavily by an additive random noise $n(t)$:

$$f(t) = s(t) + n(t) \quad 3.1$$

Let the rms voltage signal-to-noise ratio be defined:

$$\frac{S}{N} \frac{s_{\text{rms}}}{n_{\text{rms}}} \quad 3.2$$

If the signal-to-noise ratio is poor, it will be impossible to detect the information carrying signal $s(t)$ without further processing. In Figure 3.1, a 1 V 100 Hz sinusoid is masked heavily in a $2.5 \text{ V}_{\text{rms}}$ white Gaussian noise signal. As expected, with a signal-to-noise ratio of .2828, it is impossible to detect the 1 V sinusoid in the time domain.

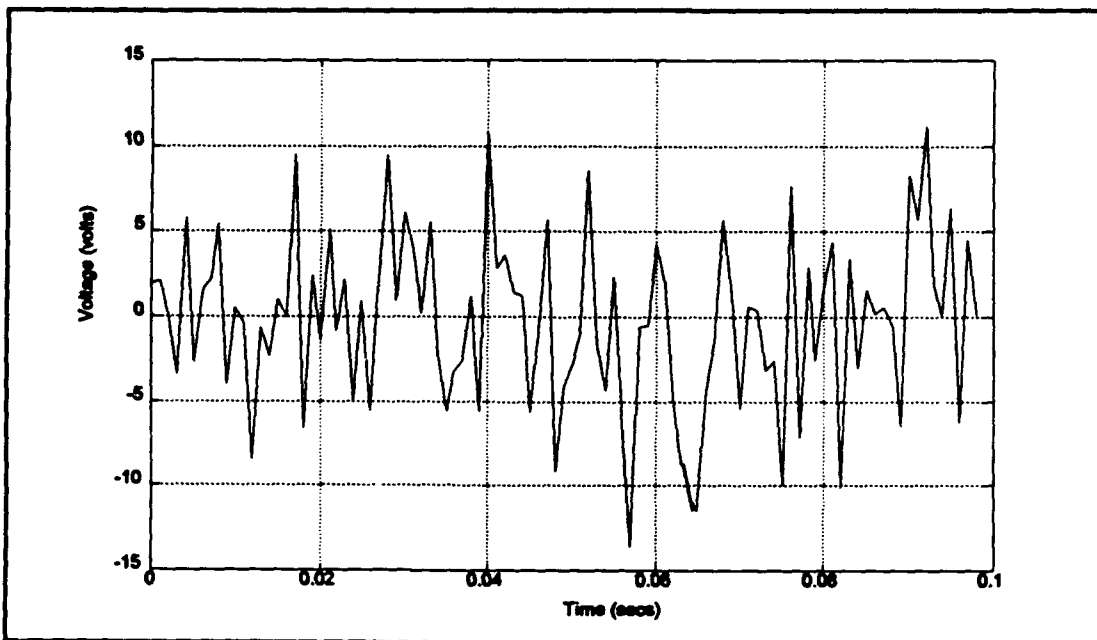


Figure 3.1-A 1 V 100 Hz sinusoid masked in $2.5 \text{ V}_{\text{rms}}$ of white Gaussian noise

Even if we transform this signal to the frequency domain, it remains impossible to detect the original sinusoid. Looking at Figure 3.2, the spectral lines of the original signal could be at 420 Hz or could be at 80 Hz. From one estimate, there is no way to predict that the spectral component of this signal actually existed at 100 Hz. The signal-to-noise ratio must be improved in order to

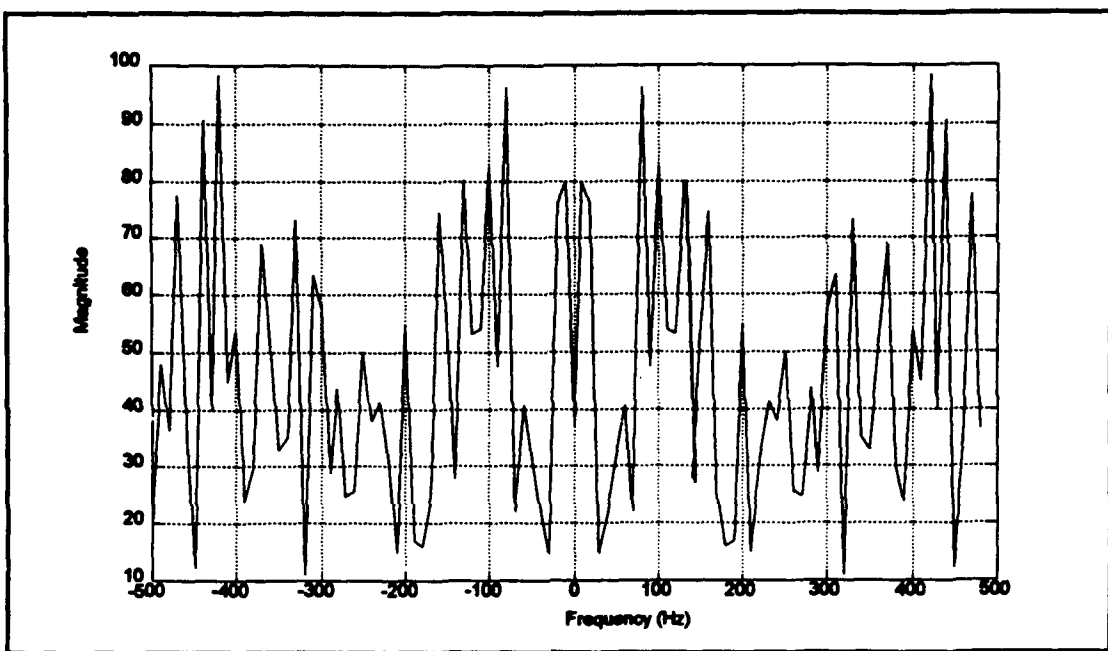


Figure 3.2-The Magnitude Spectrum of the noise corrupted sinusoid (1 record)

extract the information from the original sinusoid.

3.2 Partitioning the Signal

The first step in the ensemble average is to break the original signal into smaller, mutually exclusive time records. If a signal is sampled at a frequency f_s , for a total time T , the number of points in this time series is:

$$N_{\text{points}} = T \cdot f_s \quad 3.3$$

and the resolution in the frequency domain using a rectangular data window (Stremler 139) will be:

$$f_{\text{res}} = \frac{1}{T} \cdot \text{Hz} \quad 3.4$$

To partition the signal, a record length, t_{rec} , must be chosen. The number of records then, will be:

$$N_{records} = \frac{T}{t_{rec}} \quad 3.5$$

Each record will contain ($P_{rec} = N_{points}/N_{records}$) points.

Consequently, record number (n) contains the following points from the original series:

$$[(n-1) \cdot P_{rec}] \text{ to } [(n \cdot P_{rec}) - 1]$$

where n is the record index, and where the points in the original sequence are referenced from 0.

After the original series is partitioned, the magnitude of the Fast Fourier Transform for each record is computed and stored. Since the records are shorter than the original time series, the resolution in the frequency domain will diminish by a factor of $N_{records}$.

3.3 The Averaging Process

Each of the individual short, frequency domain estimates, or spectral records, have the same signal-to-noise ratio as the original long time series. Taken separately, each spectral record is of no more use than the original series. If the records are ensemble averaged together though, the signal-to-noise ratio improves approximately as the square root of the number of averaged records (See Section 3.4). As seen in Figure 3.3, after

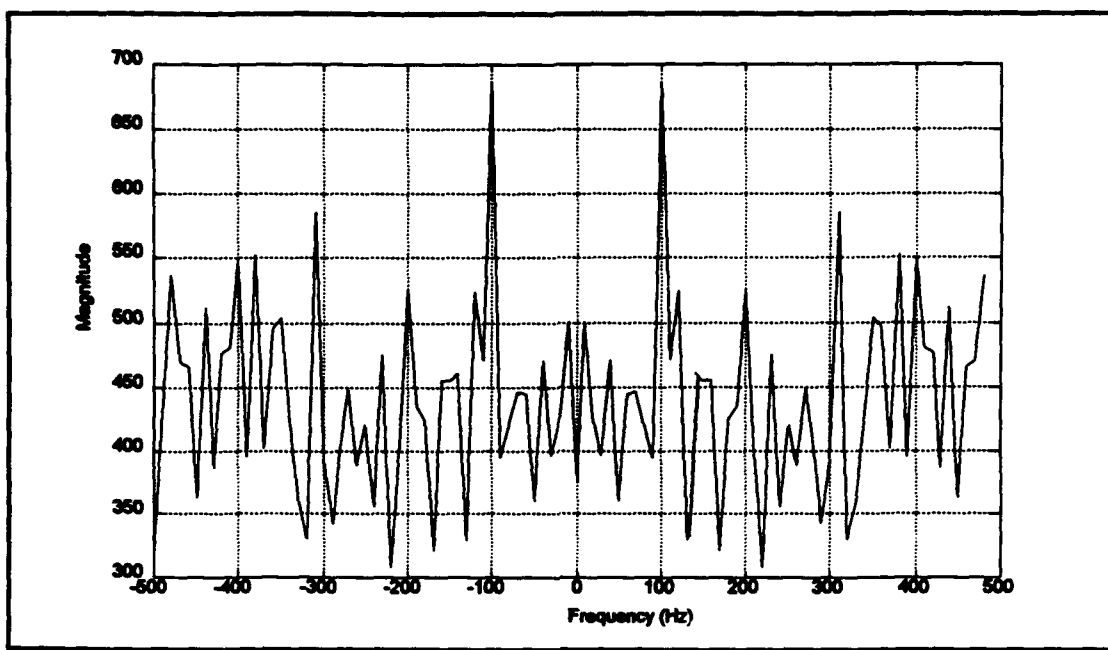


Figure 3.3-The magnitude spectrum of the noise corrupted sinusoid (10 records averaged)

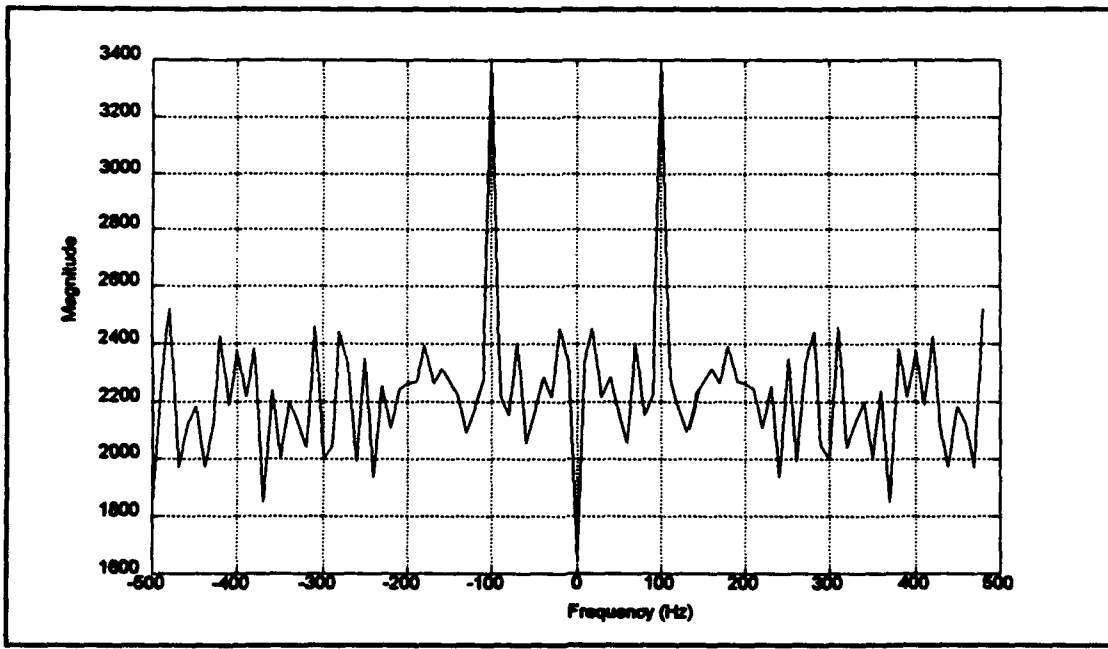


Figure 3.4-The magnitude spectrum of the noise corrupted sinusoid (50 records averaged)

averaging 10 records together, the signal-to-noise ratio has significantly increased. It is now possible to detect the original spectral lines at 100 Hz. After 50 records are ensemble averaged, there is no doubt that the original signal existed at 100 Hz. We can be more than 99% sure that the original signal existed at 100 Hz (See Section 5.2).

Although the human mind has the uncanny ability to perform precise filtering, it does not have the capability to time average. Consequently, the computer is an ideal tool to perform this averaging algorithm. It is important to note that the magnitude of the frequency spectrum must be used in the averaging process. It is impossible to average in the time domain because both the period and phase of the ICS are unknown. Taking the magnitude prevents phase cancellations from occurring in the frequency spectrum.

For a fixed total data length, segmentation and the ensemble averaging process have their trade-offs. An increase in signal-to-noise ratio can only be achieved at the expense of reduced frequency resolution. If the original series is longer than necessary to resolve any two required frequencies, then segmentation is possible and averaging is an excellent method of improving the signal-to-noise ratio.

3.4 Improving the Signal-to-Noise Ratio

During the ensemble averaging, the amplitude of the spectral lines due to the original signal increase proportionally. By representing the noise in each spectrum as an independent random variable, the central limit theorem(Peebles 118) describes their sum. It dictates that the sum of the random variables will be approximately Gaussian(Peebles 44) in distribution with the following properties:

1. The mean will be equal to the average of the noise signal (approximately zero).
2. The standard deviation, which is commensurate to the RMS noise voltage value in the spectrum, will be proportional to the square root of the number of records averaged.

Consequently, the signal-to-noise ratio in the ensemble averaged spectrum grows approximately as the square root of the number of records averaged.

Chapter 4

Processing the Power Signal

The goal of this project was to find rugged signal features that could be used to distinguish between a pump working with a good impeller and a pump working with an eroded one. The previously developed signal processing techniques were tools used to achieve this goal. Used in conjunction with more routine procedures, such as the Fast Fourier Transform, and window carpentry(Hush 155), the power data were processed to retrieve the required information.

4.1 The Initial Analysis

The first step in the analysis was to examine the frequency spectra of the signals corresponding to both a good impeller and an eroded one. Figure 4.1 illustrates a sample of each type of spectrum. The signal-to-noise ratios of the original power signals were extremely poor. Although there seemed to be signal peaks in the good impeller spectrum that did not exist in the eroded impeller spectrum, these could have been due to the variance of the noise. They were not statistically significant.

In order to increase the frequency resolution at the lower frequencies, both the sampling frequency and record lengths were modified. As mentioned before, the record

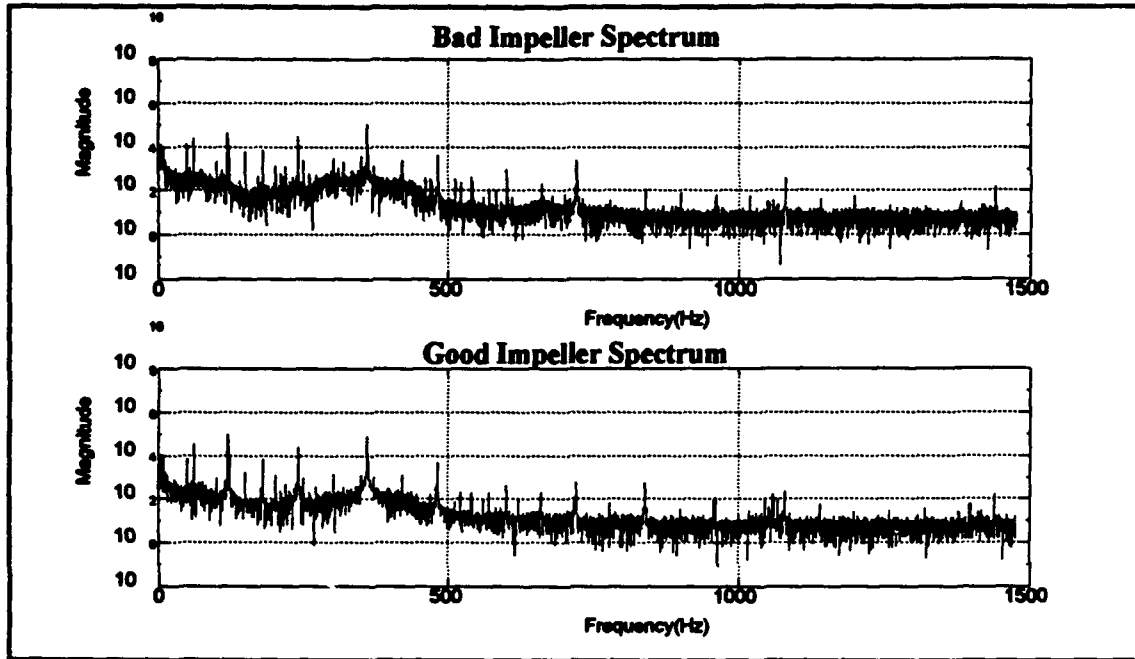


Figure 4.1-Magnitude spectra for power signals produced by both a good impeller and an eroded impeller

length is inversely proportional to the frequency resolution. The sampling frequency determines the highest frequency component that can be independently determined. This frequency, known as the Nyquist frequency, is equal to one half of the sampling frequency. Before resampling the digital data, the data were low-pass filtered at the Nyquist frequency to prevent aliasing from occurring. A tenth order digital Butterworth filter(Hush 285) was designed and implemented to accomplish this.

Since the original time series were two minutes in duration, the best possible frequency resolution was $1/120$ Hz. To gain this resolution though would have entailed computing a 720,000 point Fast Fourier Transform. This would require more than seven million complex calculations,

and would not lead to any improvement in the signal-to-noise ratio! This was not a viable option. A compromise had to be made between both the frequency resolution and the size of the FFT. As the frequency resolution increased, the size of the FFT had to decrease. The compromise resulted in a 30000 point transform with 0.2 Hz resolution. Even with the increased resolution at the lower frequencies, the signal-to-noise ratio remained too poor to detect any rugged signal features.

Next, the window carpentry was explored in order to possibly enhance the signal. The finite time sampling of a signal can be viewed as an infinite time sampling multiplied by a finite shaped window. The samples outside the window are set to zero. This product in the time domain is transformed into a convolution process in the frequency domain (denoted by a *).

$$F(\text{signal}(t) \cdot \text{window}(t)) = \frac{1}{2\pi} \cdot \text{Signal}(\omega) * \text{Window}(\omega) = \frac{1}{2\pi} \cdot \int_{-\infty}^{\infty} \text{Signal}(u) \cdot \text{Window}(\omega - u) du \quad 4.$$

The normal sampling process naturally employs the use of a rectangular shaped window (Figure 4.2). After convolving the window spectrum with the spectrum of the original signal (Figure 4.3), the energy tends to leak into the neighboring frequencies (Hush 155). If there is information contained in two neighboring frequencies with significant differences in magnitude, information can be lost. As the

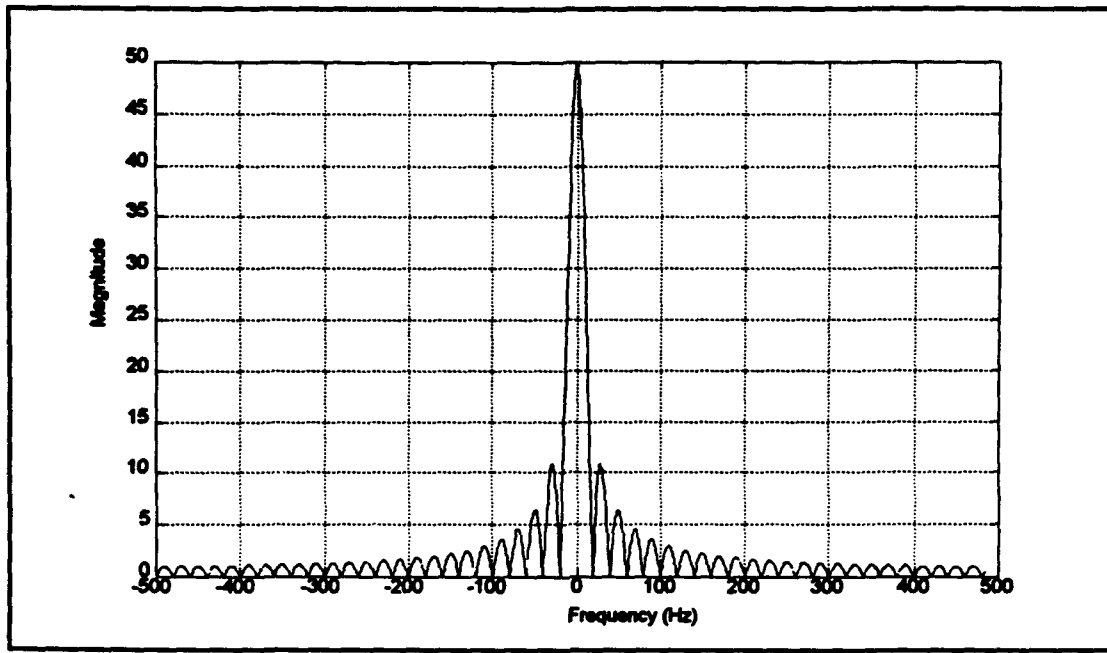


Figure 4.2-The magnitude spectrum of a 0.05 sec rectangular window

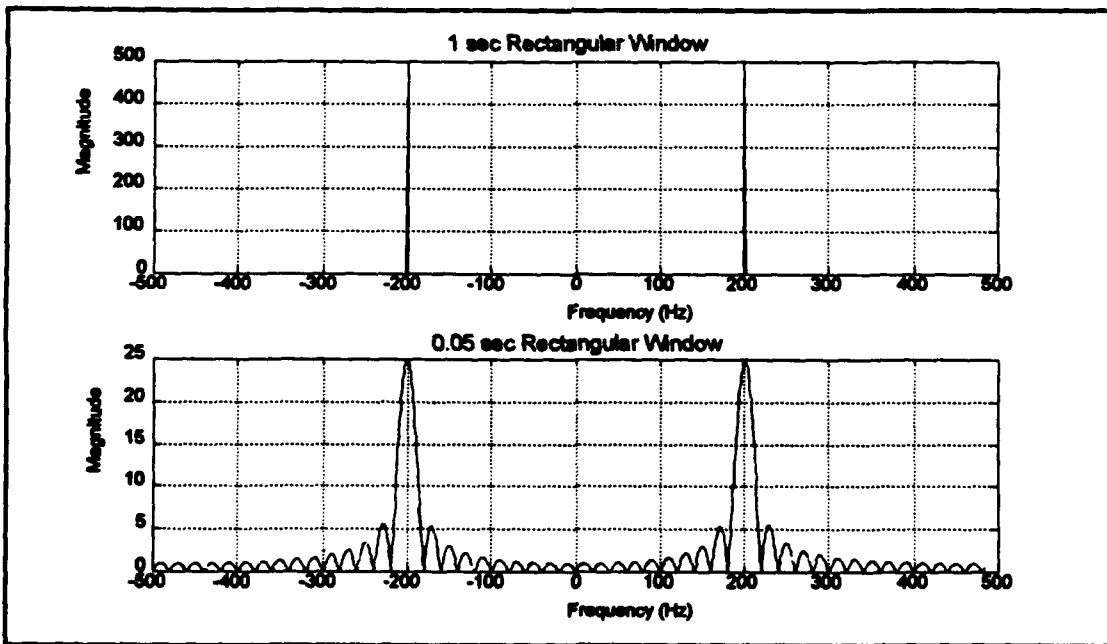


Figure 4.3-The leakage effects of the rectangular shaped window upon a 200 Hz Sinusoidal Signal

window length increases in the time domain, the leakage of energy becomes smaller in the frequency domain. This leakage is directly related to the frequency resolution. It is imperative to adjust the window length, or record length, to obtain the proper resolution.

Other types of windows such as the Bartlett, Blackman, and Kaiser windows (Hush 155) were also applied to the data. These windows tend to increase the width of the main lobe, while reducing the amplitude of the minor lobes. In application they did not act to enhance the signal. Consequently, all further data analysis was done using the natural rectangular window.

4.2 The Application of Ensemble

Averaging to the Undemodulated Spectrum

After the initial analysis, it became evident that an underlying problem was the extremely poor signal-to-noise ratio. With a ratio this poor, it would be impossible to find any rugged signal features from one record. In order to improve the signal-to-noise ratio, the process of ensemble averaging was employed on the amplitude spectrum of the undemodulated data.

Figure 4.4 shows the effect of the averaging process on

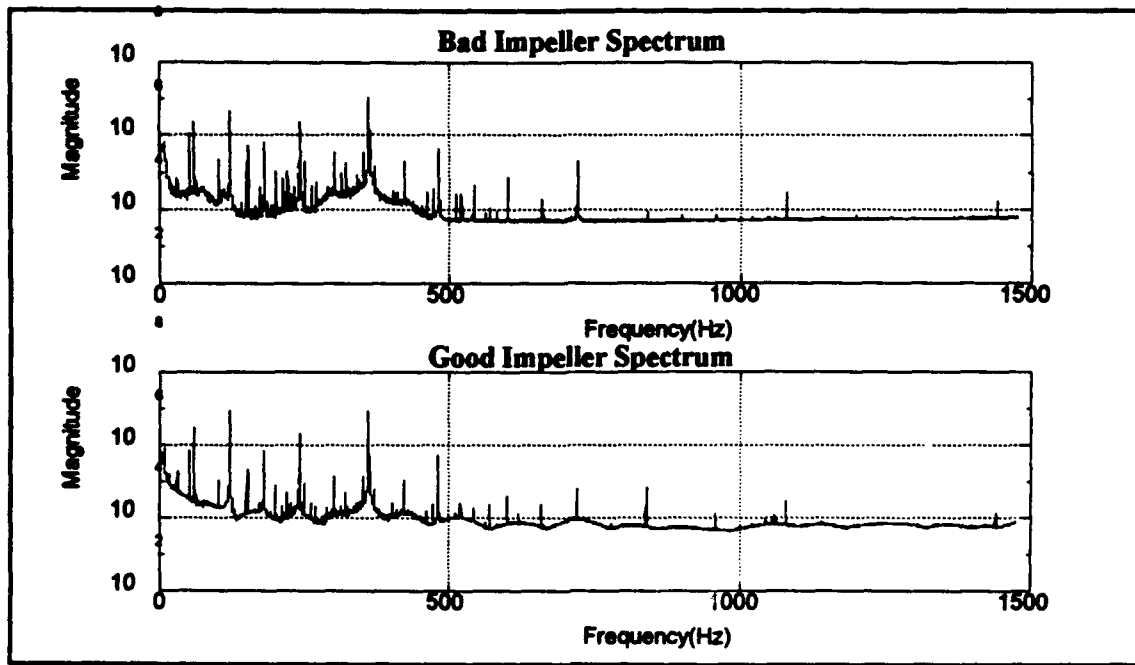


Figure 4.4-The magnitude spectra of samples ensemble averaged 24 times

the undemodulated spectra shown in Figure 4.1. After ensemble averaging 24 records together, the signal-to-noise ratio increased by approximately a factor of 5. Now that the variance in the noise had been significantly reduced, the spectral peaks could be considered reliable. As we had hypothesized, there seemed to be some type of modulating process involved. This was evidenced by the sidebands associated with the spectral lines at 60 Hz, 120 Hz, 180 Hz, 240 Hz, and 360 Hz. At this point we decided to digitally demodulate the power data in order to enhance this aspect of the signal.

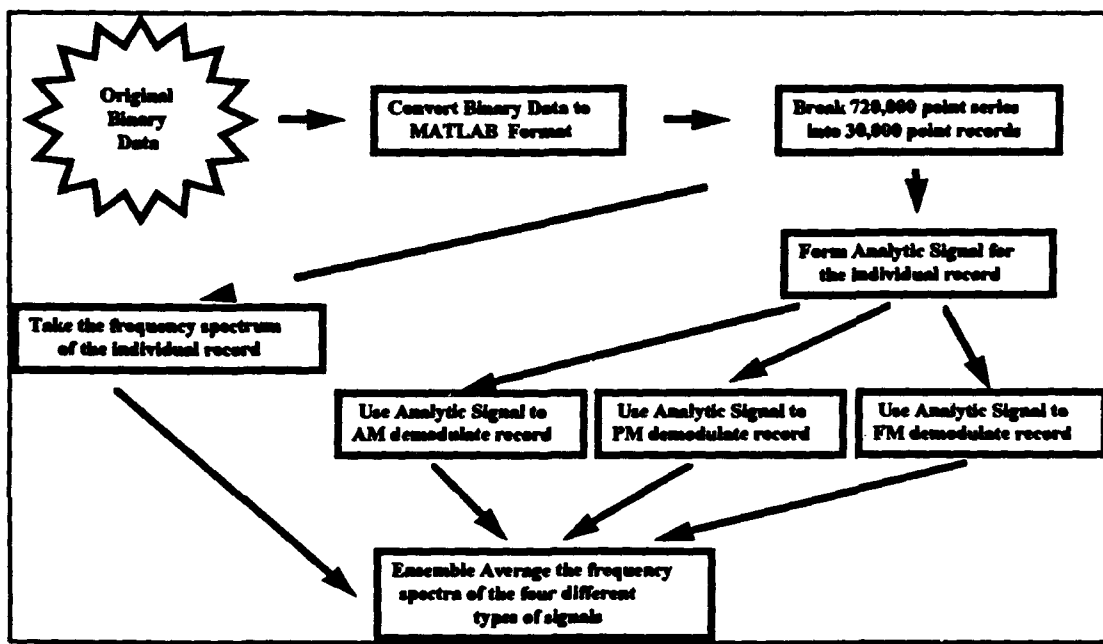


Figure 4.5-The signal processing algorithm

4.3 The Application of the Analytic Signal

As mentioned before, this eroded imeller condition can be viewed intuitively as a modulation process. In order to enhance this feature, the analytic signal was formed from the original power signal. Using both the analytic signal and the process of ensemble averaging, the signal processing scheme illustrated in Figure 4.5, was developed and implemented. The algorithm involves breaking the original two minute time series into 24, 5 sec time records. Both the frequency spectrum and analytic signal were then formed from each of the individual records. The analytic signal was further used to AM, PM, and FM demodulate the power

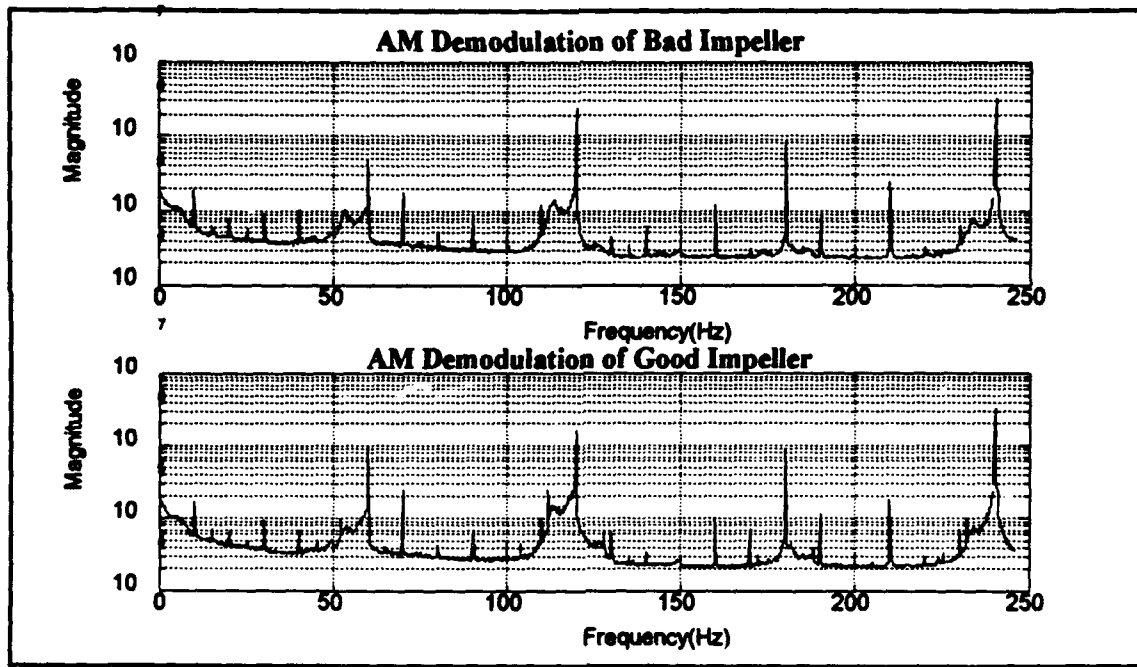


Figure 4.6-The AM demodulated magnitude spectra ensemble averaged 24 times

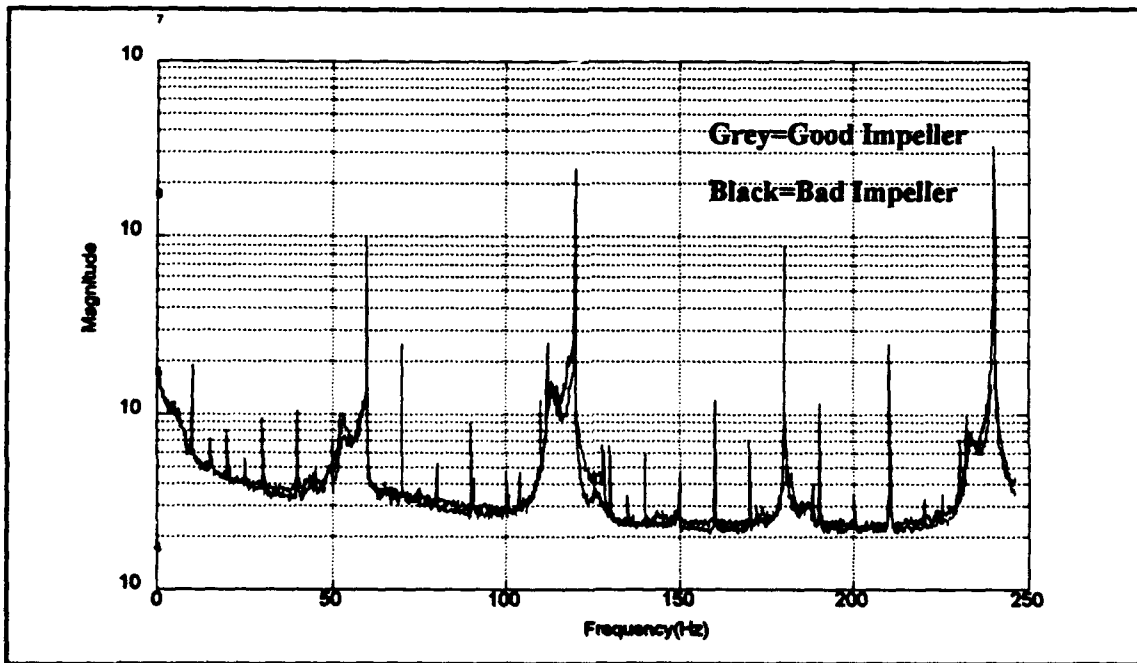


Figure 4.7-The ensemble averaged AM demodulated spectra overlayed

data. Finally, each of the different types of spectra were ensemble averaged 24 times to improve the signal-to-noise ratio.

This scheme was applied to all of the original power data. Figure 4.6 depicts the results of the AM demodulation process. Not only did the processed data have a reliable signal-to-noise ratio, there seemed to be spectral lines that were enhanced by the demodulation process. This information could possibly help to distinguish between the two conditions. Similar results occurred in both the PM and FM demodulated spectra.

The results were even more promising when the two spectra were overlayed(Figure 4.7). At certain frequencies there were significant energy differences between the two spectra. From an initial inspection of the different samples, the disparities seemed to be statistically significant. In other words, all the spectra of a certain condition exhibited the same characteristics. Similar energy differences existed throughout the other demodulated spectra.

The signal processing scheme seemed to have worked; the application of the analytic signal was the key. It extracted information from the original signals that could possibly be used to predict the pump's condition. It was then time to enter the final phase of the project, namely the classification stage.

Chapter 5

Determination of the Pump Condition

After a cursory examination, the information extracted through the signal processing algorithms appeared to be rugged. In other words it was statistically significant and could be used to classify the data. This hypothesis though, had to be put to the test. In order to determine the condition of the pump, two classification techniques were employed; the nearest neighborhood technique and a neural net known as the perceptron.

5.1 Pinpointing the Rugged Signal Features

The first step in predicting the pump condition was to choose the rugged signal features that could be used to distinguish between a signal produced by a good impeller and a signal produced by an eroded one. Again, rugged means the feature is statistically significant, and could be reproduced during different trials. The first test was to determine if the process was stationary(Stremler 500).

Tests were conducted using the same impeller under the

same conditions at different times. Although the background noise level shifted slightly, the shapes of the demodulated spectra remained identical. This suggested that the pump process itself was stationary.

The next step was to find features that were common to a certain condition and that could be used to differentiate it from the other condition. To find these, a good and a bad set of templates were formed. A template was created by taking the already ensemble averaged spectra of a given condition and ensemble averaging them together again. For instance, to form the good FM demodulated template, the ensemble averaged FM demodulated spectra from all the good samples were averaged together again. Templates were formed for the original spectrum, and the AM, PM, and FM demodulated spectra. Thus, there were both four good, and four bad templates. These templates provided a visual representation of the average signal produced from a pump working with a good impeller, and the average signal produced from a pump working with an eroded impeller.

The four sets of corresponding templates were compared, and examined for significant differences in energy. Since, the background noise levels were virtually equal, the signal peaks could be compared directly. The frequencies at which these energy differences existed were designated as possible rugged signal features. A criterion now had to be created to determine whether or not these energy differences could

be considered rugged.

5.2 The 1% Test

The test developed to determine whether or not a signal feature was rugged was the 1% test. To pass the 1% test, there had to be less than a 1% chance that the difference in energy at a certain frequency was due to the variance of the noise. In other words there had to be more than a 99% chance that the energy difference was due to the information and not due to the noise.

The development of the 1% test centers around the Central Limit Theorem. The Central Limit Theorem states that the sum of a large number of independent random variables approaches a Gaussian distribution. The noise in the different time records can be described by an independent random variable. Consequently, the Central Limit Theorem pertains to the ensemble average of the individual records. In the limit as the number of records approaches infinity, the distribution of the noise will become Gaussian.

Since, each of the spectra was ensemble averaged 24 times, the distribution of the noise was assumed to be Gaussian. To apply the 1% test, the difference in the energy peaks was calculated at each possible rugged signal feature. If the probability were less than 1% that the difference was due to the noise, then the signal feature was

considered rugged. Figure 5.1 shows the good and bad AM demodulated templates overlayed. The marked frequencies easily passed the 1% test, and were five of the rugged signals features used to classify the data. Using this criterion, 26 rugged features were found throughout the four sets of templates. The specific breakdown of signal features was as follows:

- 2 from the original spectrum template
- 4 from the AM demodulated template
- 8 from the PM demodulated template
- 15 from the FM demodulated template

Total: 29 rugged signal features

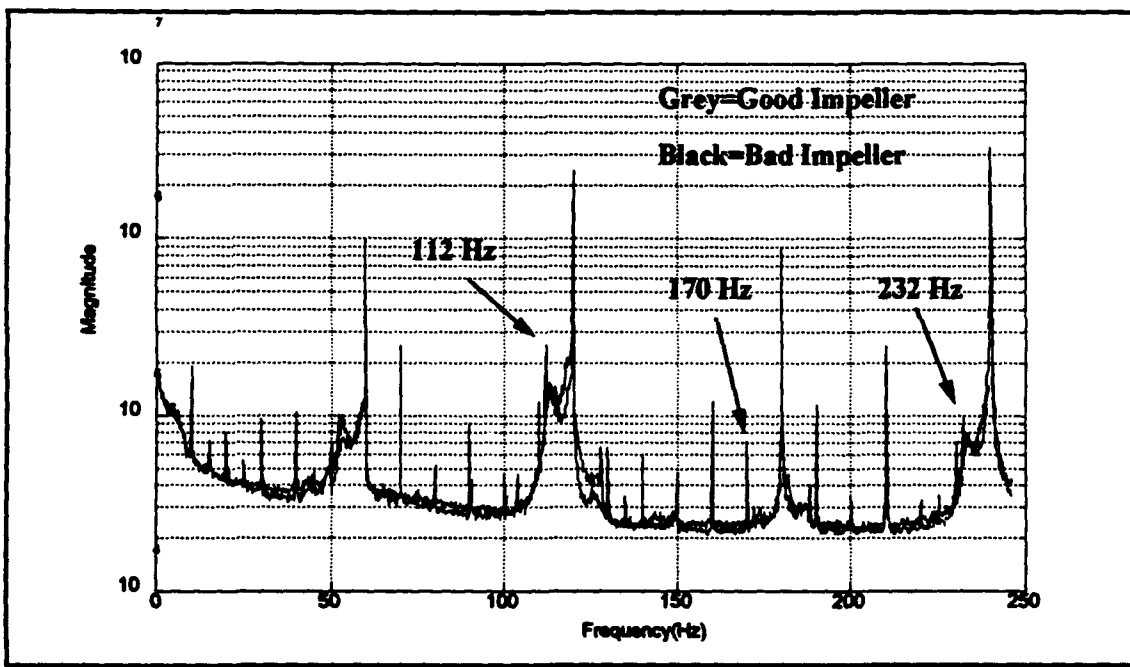


Figure 5.1-The good and bad AM demodulated templates overlaid

5.3 The Moving Average Filter

It is one thing to be able to identify the rugged signal features visually, but the computer needs a method by which to quantify them. Although the 1% test provided a criterion to determine if a signal feature is rugged, it did not provide a method by which to quantify it. To accomplish this, a low-pass moving average filter was developed. Basically, the moving average filter would compare the area beneath a signal peak to the area beneath the noise surrounding it, producing a signal-to-noise ratio. The spectral peak width was assumed to be 0.6 Hz (This was identified visually). The area under this frequency span was compared with the neighboring 1.2 Hz of noise. Since, it is expected that the background noise level will change during pump operation, the signal-to-noise ratio is an ideal quantity to describe these features.

The moving average filter was used to measure the signal-to-noise ratios throughout the four spectra of each sample. Consequently, each power data sample had 29 signal-to-noise ratios associated with it. Figure 5.2 shows the filter set on the 170 Hz frequency. To compute the signal-to-noise ratio, the area beneath the signal in the white box, was compared with the area beneath the background noise in the grey boxes. The corresponding signal-to-noise ratios from the good and bad samples would later be compared to help predict the pump's condition.

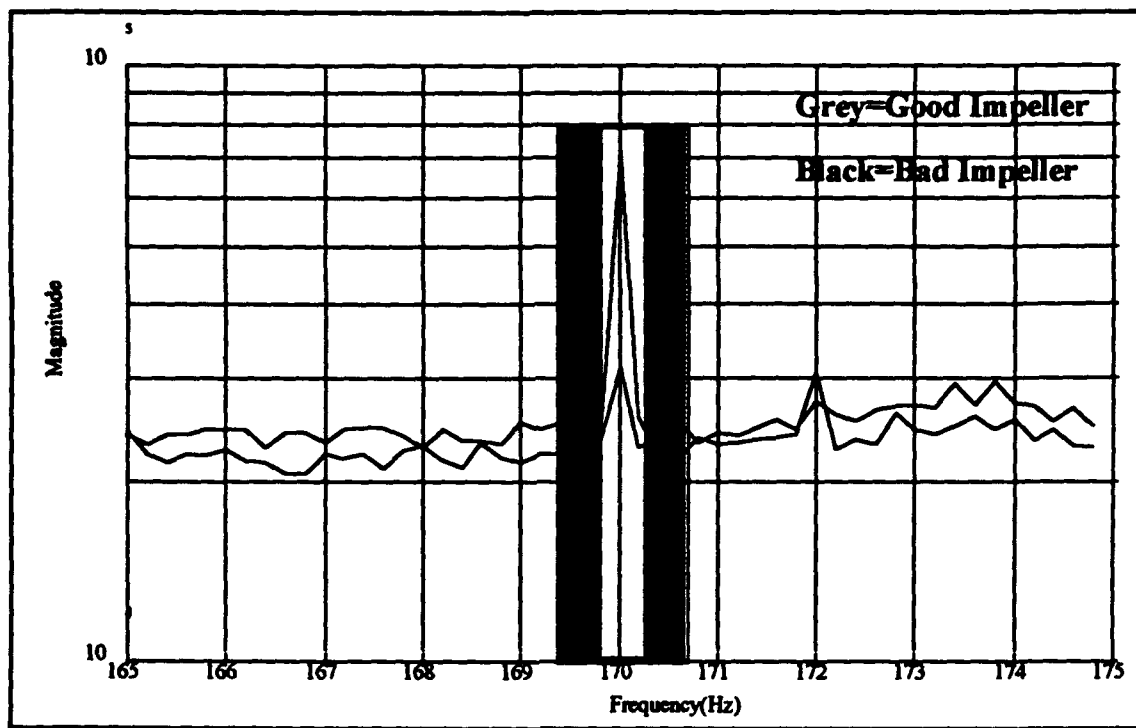


Figure 5.2-The moving average filter centered on the 170 Hz spectral line

5.4 Creating the Pattern Vector

Now that the rugged signal features had been quantified, it was time to establish a pattern for each sample. This pattern would be formed from the 29 signal-to-noise ratios calculated for each sample. Each signal-to-noise ratio would serve as a component of a 29 dimensional pattern vector. This pattern vector would act as a fingerprint for each individual sample. It would be this fingerprint that would later be used to classify the pump condition that created it.

In this instance the pattern vectors consisted of components with identical units (W/W). This need not be the

case. Under different circumstances, one component could have units of volts while another has units of amps. The important aspects of the vector are that the order of the components remain constant and that the components are calculated in an analogous fashion.

5.5 The Nearest Neighborhood Technique

Once the pattern vectors had been formed for each of the individual samples, it was time to apply them to a classification routine. The first scheme implemented was the nearest neighborhood technique(Kapouleas 177). This procedure involved comparing the sample test pattern vectors with the average good and the average bad pattern vectors.

The first step was to create the average good and bad pattern vectors. To accomplish this two sets of templates were formulated using a training set. The training set consisted of samples whose classification was previously known by the computer. Using the training set, the four distinct templates were created for both the good impeller and the eroded impeller. The moving average filter was implemented to quantify the previously determined rugged signal features. Then, both the average good and the average bad template vectors were created using these signal-to-noise ratios.

After creating the template pattern vectors, the test set was applied to the classification scheme. The test set

consisted of pattern vectors whose condition was unknown to the computer, and that were not involved in the formation of the templates. The mean squared distance (D) between the test pattern vector and each of the template vectors was calculated using the following formula:

$$D = [(a(1) - b(1))^2 + (a(2) - b(2))^2 + (a(3) - b(3))^2 + \dots + (a(n) - b(n))]^{0.5} \quad 5.1$$

The test vector was then classified as the template vector that produced the smaller distance value (D).

The nearest neighborhood technique can also be perceived visually. Figure 5.3 is a visual representation of a three dimensional vector space, as opposed to the 26 dimensional vector space that was actually created. In this space each dimension represents a component of the pattern

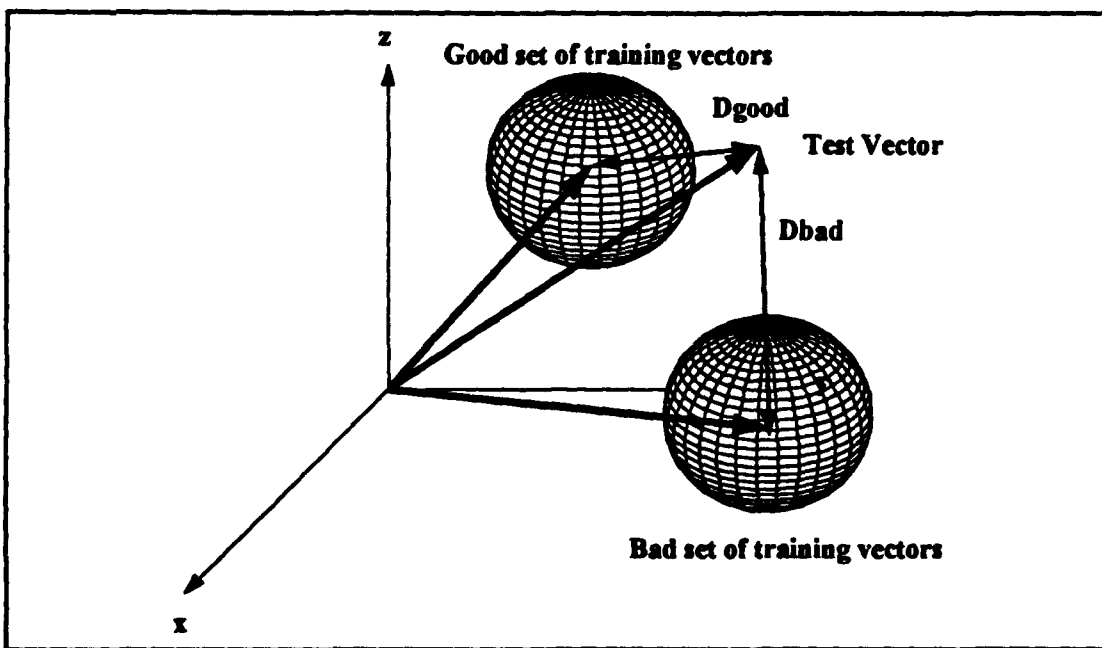


Figure 5.3-A three dimensional vector space

vector. One sphere represents the volume over which the good set of training vectors was located, while the other sphere represents the volume over which the bad set were located. The vectors drawn to the center of each sphere correspond to the good and bad template vectors. The mean squared distance was then calculated from the test vector to each of the template vectors. In this case the test vector was closer to the good template vector and would be classified as a signal produced from a good impeller.

It is important to note that the nearest neighborhood technique weights each of the individual components of the pattern vector equally. Using this technique, 90% of the test set was classified correctly. Even in the worst case where the system broke down, 19 of the 29 individual components were classified correctly. This led to the hypothesis that weighing the components differently would lead to a higher classification efficiency.

5.6 The Perceptron

In order to weight the individual components differently, a simple neural net known as a perceptron (Kosko 187) was implemented. The structure of the perceptron can be seen in Figure 5.4. The perceptron multiplies each of the individual components of the pattern vector by a specific weight. These weighted components are added

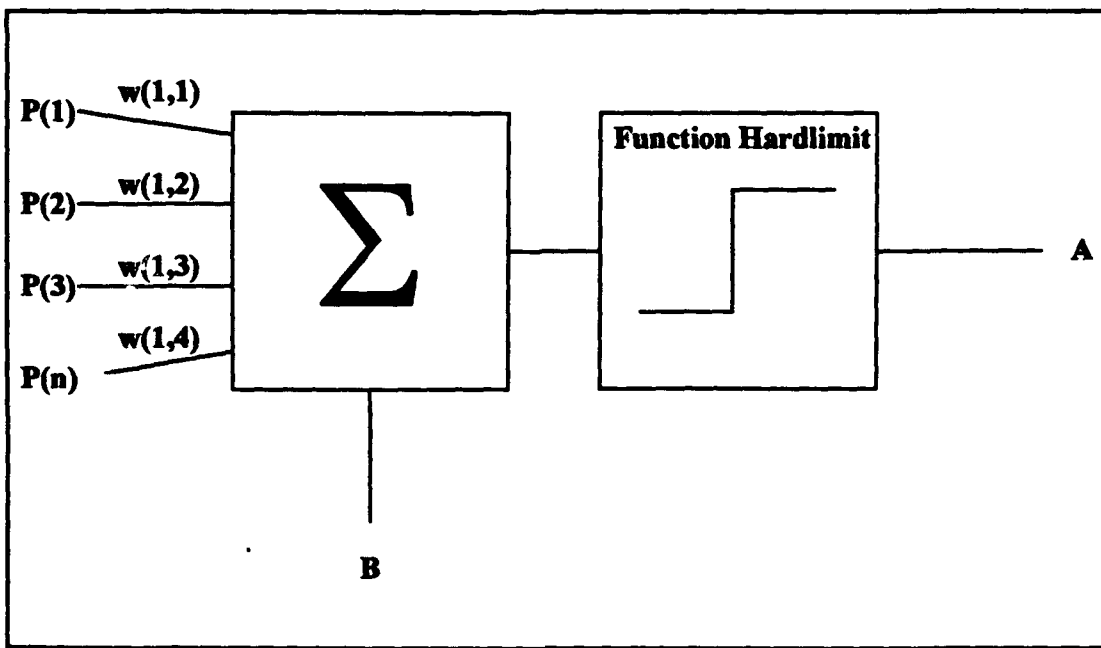


Figure 5.4-The perceptron

together and then added to an offset B . The function hardlimit is equal to 1 when the input is greater than 0 and equal to 0 when the input is less than or equal to 0. Consequently, when the total sum is greater than 0, the neuron fires producing a value of $A=1$. If the total sum is less than 0, then the neuron does not fire producing a value of $A=0$. The perceptron was designed to produce a value of $A=1$ for a good impeller, and a value of $A=0$ for an eroded impeller.

The weights and offset B are calculated in a recursive training process following an established learning rule. To train the neuron though, it first must be initialized. This is done by setting the weights and the offset to small random values. This provides enough variation in the neuron to take advantage of the learning rule. A batch of training

vectors are then applied to the perceptron. Again, the training set consists of samples whose classifications are known to the computer. The weights and offset are adjusted until all members of the training set are classified correctly. The following rule is used:

Case (1) If after the presentation of a training vector, the output of the neuron is correct, the weights and offset remain unchanged.

Case (2) If the output of the neuron was a 0 and should have been a 1, the weights are increased by the value of the individual components of the training vector, and the offset is increased by 1.

Case (3) If the output of the neuron was a 1 and should have been 0, the weights are decreased by the value of the individual components of the training vector, and the offset is decreased by 1.

Following this rule it took approximately 100,000 recursions to train the perceptron. It is important to note that 100% classification of the training set can only be achieved if the vectors are linearly separable. Otherwise, a more complex neural network must be employed.

It was now time to apply the test set. Again, the test set consisted of samples whose classification was unknown to the computer, and that were not involved in the training process. Using the trained perceptron 100% of the test set was classified correctly. By simply shifting the weights of

the individual components it was possible to raise the classification efficiency from 90% to 100%. Thus, the objectives of the project had been met. The signal processing routines and classification techniques had been developed to diagnose the eroded impeller condition.

The Future

In the past, a pump would have had to been shut down and taken apart to be examined. Due to their location, certain pumps could never be monitored under normal circumstances. In the worst case, the fault may have led to a complete system shut down and a prolonged stay in dry dock. These algorithms are the basis for a non-invasive monitoring system that removes this risk. Currently, with a power meter, an analog-to-digital converter, a computer, and 15 minutes of computation, a pump can be monitored for the eroded impeller condition. In the future the system will be expanded to include more phases of pump operation.

This is only the beginning of the project. Although the basic algorithms have been created, they would most likely have to be fine tuned to fit each submarine. This will require more data and research. This project will also expand to encompass more aspects of pump operation. This will entail the classification of other fault conditions that will include, but will not be limited to:

- (1) cavitation
- (2) impeller nut back-off, and
- (3) mechanical seal leakage

Eventually, this system will provide the Navy with an efficient and inexpensive method for the complete monitoring of all pump operation.

Works Cited

- Hertz, John, Anders Krogh, and Richard Palmer. Introduction to the Theory of Neural Computation. California: Addison-Wesley Publishing Company, 1991.
- Hush, Don and Samuel Sterns. Digital Signal Analysis. New Jersey: Prentice Hall, 1990.
- Jenkins, Gwilym and Donald Watts. Spectral Analysis and its applications. California: Holden-Day, 1968.
- Kapouleas, Ioannis and Sholom Weiss. "An Empirical Comparison of Pattern Recognition, Neural Nets and Machine Learning Classification Methods." Readings in Machine Learning. Ed. Jude W. Shavlik and Thomas G. Dietterich. California: Morgan Kaufmann Publishers, 1990: 177-183.
- Kosko, Bart. Neural Networks and Fuzzy Systems. New Jersey: Prentice Hall, 1992.
- Munson, Bruce, Donald F. Young, and Theodore H. Okiishi. Fundamentals of Fluid Mechanics. New York: John Wiley and Sons, 1990.
- Peebles, Peyton. Probability, Random Variables, and Random Signal Principles. New York: McGraw-Hill, Inc., 1993.
- Stremler, Ferrel. Introduction to Communication Systems. Massachusetts: Addison-Wesley Publishing Company, 1990.